Electronic Supplementary Material (ESI) for ChemComm.

Supporting Information

Exploration of $Na_{2.65}Ti_{3.35}Fe_{0.65}O_9$ as anode materials for Na-ion batteries

Maowen Xu[a,b*†], Jun-Ke Hou [a,b†], Yu-Bin Niu[a,b], Guan-Nan Li[a], Yu-Tao Li[c], Chang Ming Li[a,b*]

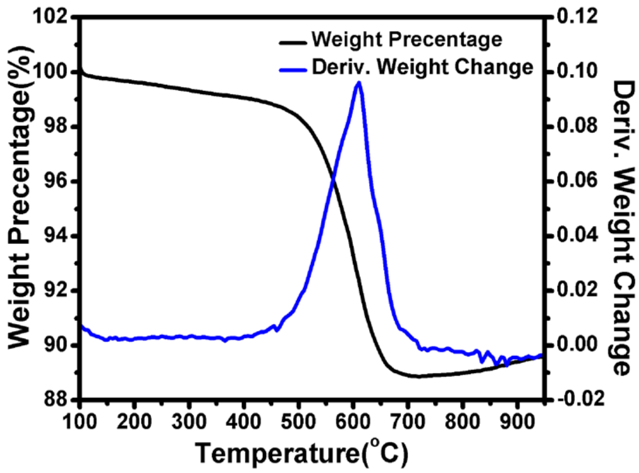

Fig.S1. TGA of precursor of $Na_{2.65}Ti_{3.35}Fe_{0.65}O_9$

The thermal properties of the obtained $Na_{2.65}Ti_{3.35}Fe_{0.65}O_9$ precursor were studied using TG analysis. Fig. S1 displays the TG curve for the $Na_{2.65}Ti_{3.35}Fe_{0.65}O_9$ precursor. It shows a first weight loss around 400°C, which is attributed to the evaporation of residual water and the removal of chemically bound water in the sample. The following sharp drop in weight above 700 °C corresponds to the decomposition of raw materials and the formation of $Na_{2.65}Ti_{3.35}Fe_{0.65}O_9$ phase. The weight loss between 700 and 900°C is very little. This behavior implies that the formation of $Na_{2.65}Ti_{3.35}Fe_{0.65}O_9$ phase is completed at this stage. So, he samples were annealed at 750 ^{o}C, 800 ^{o}C, 850 ^{o}C and 900 ^{o}C in this work.

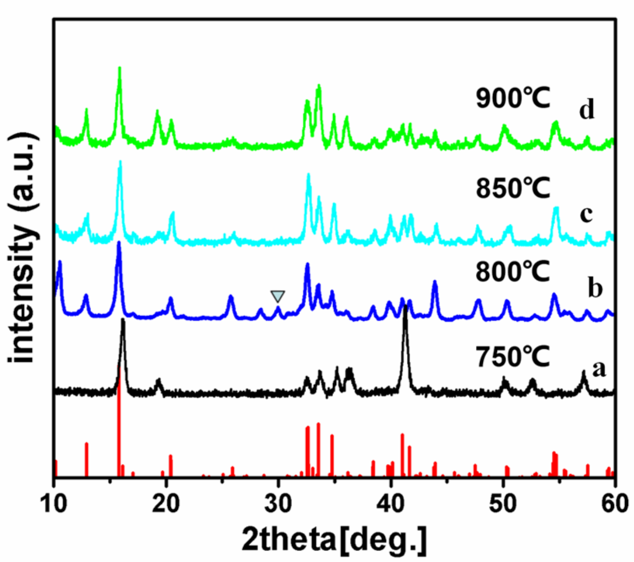

Fig.S2. XRD patterns of samples obtained at different temperature

The XRD patterns of the as-synthesized samples display in Fig.S2. The results suggested that the $Na_{2.65}Ti_{3.35}Fe_{0.65}O_9$ has been formed after sintering at 700 ^oC, and with the increasing of sintering temperature, the crystallinity of the samples increased. It is clearly that the main diffraction peaks positions of the materials obtained at 800 ^oC agree well with $Na_{2.65}Ti_{3.35}Fe_{0.65}O_9$ (PDF No.04-014-0704). However, there are still weak impurity peaks at 21.5° and 30°, it showed that the obtained product at 800 °C still contains trace amounts of impurities. After sintering at 850 °C and 900 °C, the XRD results (Fig.S2c and d) are in good agreement with isostructural $Na_{2.1}Ru_4O_9$, suggesting the formation of monoclinic phase crystal.

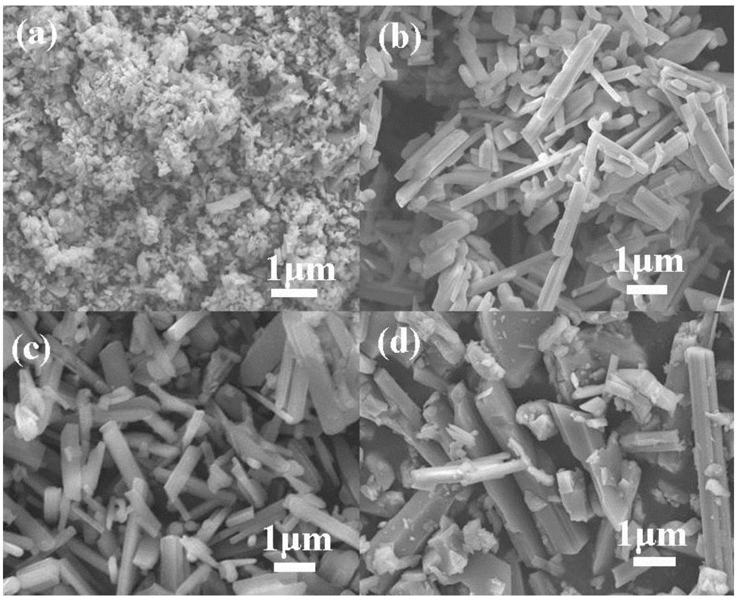

Fig. S3. SEM of the samples obtained at different temperature: (a) 750 °C, (b) 800 °C, (c) 850 °C and (d) 900 °C for 15h.

Fig.S3 shows SEM images of the four samples obtained at different temperatures. It can be observed that $Na_{2.65}Ti_{3.35}Fe_{0.65}O_9$ with rods morphology has begun to form at 800 °C; When sintering temperature increase to 850 °C, more uniform rods can be obtained. With the further increase of temperature, rods become blocks (Fig.S3d).

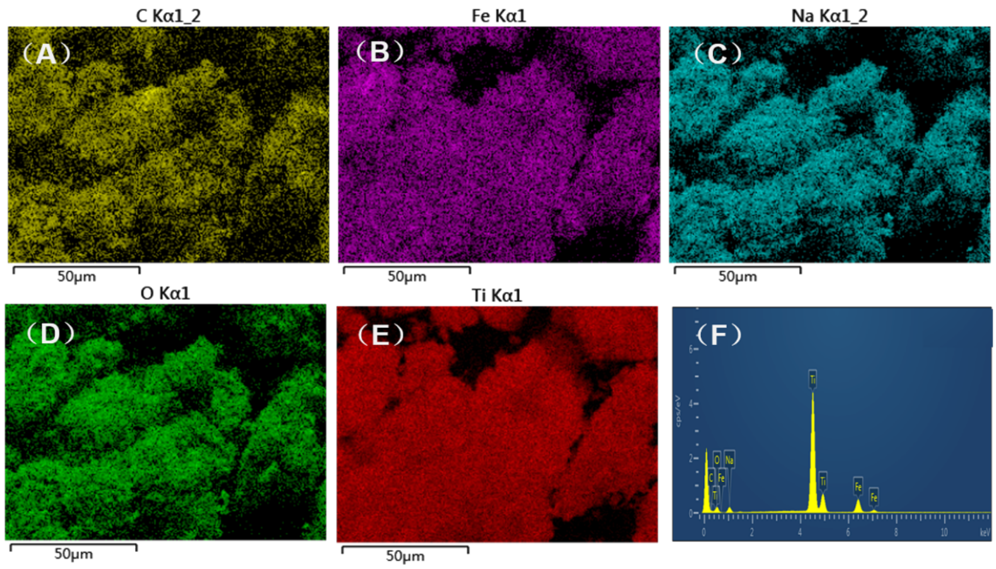

Fig.S4. EDS-element distribution mapping images of $Na_{2.65}Ti_{3.35}Fe_{0.65}O_9/C$.

The elemental mapping of carbon (Fig. S4(A)) by EDS clearly show that carbon was homogeneously distributed around the $Na_{2.65}Ti_{3.35}Fe_{0.65}O_9$ microcrystallites. The EDS elemental mapping results for other elements in the same area are shown in Fig. S4B–E. Although the carbon coating greatly contributed to the excellent rate capability of the $Na_{2.65}Ti_{3.35}Fe_{0.65}O_9$ electrode, the carbon coating effect was not significant at a low current rate which typically represents the intrinsic electrochemical performance of new cathode materials.

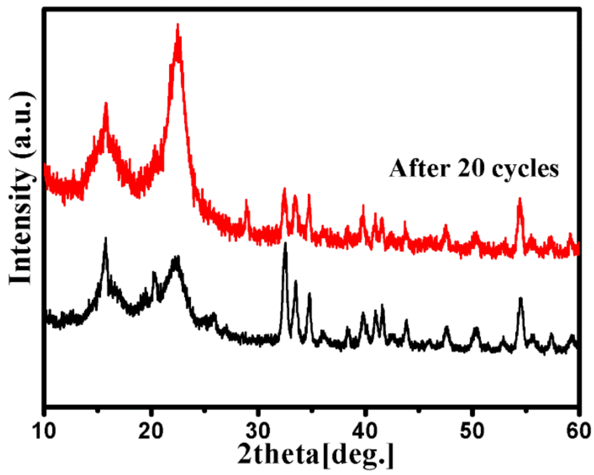

Fig.S5. Structural stability of $Na_{2.65}Ti_{3.35}Fe_{0.65}O_9$ upon cycling

The difference between XRD patterns of the pristine electrode and the sample in the discharged state after 20 cycles with a 0.5 C cycling rate was insignificant (Fig. S5), indicating good structural stability during charging/discharging. This implies that Na^+ ions are immobile in the structure and do not significantly affect the structural evolution upon cycling.